Annals of Botany **108**: 885–894, 2011
doi:10.1093/aob/mcr218, available online at www.aob.oxfordjournals.org

ANNALS OF BOTANY
Founded 1887

Leaf-traits and growth allometry explain competition and differences in response to climatic change in a temperate forest landscape: a simulation study

Mei Yu[1,3,*] and Qiong Gao[2]

[1]*Institute for Tropical Ecosystem Studies, University of Puerto Rico – Rio Piedras, PO Box 70377, San Juan, PR 00936-8377, USA,* [2]*State Key Laboratory of Earth Surface Processes and Environmental Changes, College of Resources, Beijing Normal University, Beijing 100875, P.R. China and* [3]*Institute of Botany, Chinese Academy of Sciences, Beijing 100093, P.R. China*

** For correspondence. E-mail: meiyu@ites.upr.edu*

Received: 11 January 2011 Returned for revision: 12 May 2011 Accepted: 17 June 2011 Published electronically: 10 August 2011

• *Background and Aims* The ability to simulate plant competition accurately is essential for plant functional type (PFT)-based models used in climate-change studies, yet gaps and uncertainties remain in our understanding of the details of the competition mechanisms and in ecosystem responses at a landscape level. This study examines secondary succession in a temperate deciduous forest in eastern China with the aim of determining if competition between tree types can be explained by differences in leaf ecophysiological traits and growth allometry, and whether ecophysiological traits and habitat spatial configurations among PFTs differentiate their responses to climate change.

• *Methods* A temperate deciduous broadleaved forest in eastern China was studied, containing two major vegetation types dominated by *Quercus liaotungensis* (OAK) and by birch/poplar (*Betula platyphylla* and *Populus davidiana*; BIP), respectively. The Terrestrial Ecosystem Simulator (TESim) suite of models was used to examine carbon and water dynamics using parameters measured at the site, and the model was evaluated against long-term data collected at the site.

• *Key Results* Simulations indicated that a higher assimilation rate for the BIP vegetation than OAK led to the former's dominance during early successional stages with relatively low competition. In middle/late succession with intensive competition for below-ground resources, BIP, with its lower drought tolerance/resistance and smaller allocation to leaves/roots, gave way to OAK. At landscape scale, predictions with increased temperature extrapolated from existing weather records resulted in increased average net primary productivity (NPP; +19 %), heterotrophic respiration (+23 %) and net ecosystem carbon balance (+17 %). The BIP vegetation in higher and cooler habitats showed 14 % greater sensitivity to increased temperature than the OAK at lower and warmer locations.

• *Conclusions* Drought tolerance/resistance and morphology-related allocation strategy (i.e. more allocation to leaves/roots) played key roles in the competition between the vegetation types. The overall site-average impacts of increased temperature on NPP and carbon stored in plants were found to be positive, despite negative effects of increased respiration and soil water stress, with such impacts being more significant for BIP located in higher and cooler habitats.

Key words: Succession, watershed, ecophysiological trait, landscape carbon dynamics, temperate forests, competition, simulation, *Quercus liaotungensis*, *Betula platyphylla*, *Populus davidiana*.

INTRODUCTION

Disturbance, a primary driver for secondary succession, alters both ecosystem structures and functions, and it is receiving increasing attention in global change studies (Dale *et al.*, 2001; Botta and Foley, 2002; Keane *et al.*, 2004; Beard *et al.*, 2005; Lecomte *et al.*, 2006; Field *et al.*, 2007). Impacts are not only short term, such as biomass loss immediately after fires or hurricanes, but can also last for decades or even centuries of the ecosystem succession. Recent studies have shown that the history of disturbance regimes or the legacies after disturbances may remain in effect long after the events (Turner *et al.*, 1998; Elmore *et al.*, 2006; Perry and Enright, 2006). Disturbance-induced changes in ecosystem composition/structure may amplify, suppress or even reverse the ecosystem carbon responses and feedbacks to climatic change because species patterns are altered in both space and time (Field *et al.*, 2007). Competition plays a key role in modifying ecosystem structure and this mechanism should be considered in disturbance-incorporating studies of ecosystem structures and functions across various spatiotemporal scales.

Simulation with computer models has proved efficient in addressing succession, i.e. temporal changes in ecosystem structure, and consequent changes in ecosystem functions at multiple spatiotemporal scales (Shugart and Smith, 1996; Mladenoff, 2004; Bond-Lamberty *et al.*, 2005). Gap replacement models, using individual-based approaches and mostly with stochastic algorithms, are representative of the efforts to simulate succession and consequent ecosystem functional changes (Friend *et al.*, 1993; Shugart and Smith, 1996; Bugmann, 2001). To address ecosystem changes over greater spatial extent, spatially explicit models, often in conjunction

with geographical information systems, such as the LANDIS and DISPATCH models, were also developed and are widely used (Baker, 1999; He and Mladenoff, 1999; Mladenoff, 2004; Perry and Enright, 2006).

In contrast to the individual-based approaches, most biogeochemical models, biogeographical models or their hybrids, such as MC1, BIOME-BGC, CENTURY and TESim (Parton *et al.*, 1993; Thornton, 2000; Bachelet *et al.*, 2001; Gao *et al.*, 2007), aim to model ecosystem processes and functions at the level of plant functional type (PFT) or even higher, at the biome level. Such an approach partially avoids individual-related uncertainties and parameterization, and thus expands model applications in both space and time. These models are widely applied to investigate carbon, water and nutrient dynamics, and vegetation distribution (in hybrid models), in the context of climate change and various natural and anthropogenic disturbances. However, given the increasingly intense and extensive human disturbance, such as land-use changes, and the well-documented frequent natural disturbances, it is necessary to investigate whether PFT-based models can successfully simulate disturbance-induced temporal changes in ecosystem structure in order to provide scientifically sound predictions under global change scenarios. In particular, whether and how plant functional traits embedded in these models can explain ecosystem succession deserve further investigation.

Simulation modelling also makes it possible to investigate changes in various ecosystem processes induced by external forces and to project the synthetic ecosystem responses to driving forces (Field *et al.*, 2007; Luo, 2007). For example, increased temperature in temperature-limited areas may influence carbon storage in opposite ways, by improving carbon assimilation and nutrient decomposition, which favour carbon storage, and by accelerating vegetation and heterotrophic respiration, which otherwise reduce carbon storage. The interactions between biogeochemical processes and biogeographical patterns make the responses and feedbacks of ecosystems to climate change even more complicated. Recent reviews have discussed the positive and negative feedbacks of ecosystems to climate change and emphasized the importance of more complete and integrated modelling (Luo, 2007). Spatially explicit models, especially spatially interactive models capable of simulating lateral flows and processes, make it possible to investigate the interactions between vegetation distribution patterns and ecosystem processes and consequent integrative responses to climate change (Mladenoff, 2004).

Temperate forests are important for carbon sequestration in China, yet remain a focal region for forest restoration (Chen, 1997; Fang *et al.*, 2006). Primary forests in this area have been destroyed over the long history of agricultural development. Studies on secondary succession after severe human disturbances started in the 1980s (Chen, 1997). The well-known successional path following disturbance is that small broadleaved deciduous trees (*Betula* and *Populus*) appear at the early stage of succession as a pioneer functional type because of their fast growth under relatively high soil water availability. As succession proceeds, this functional type gradually gives ways to slow-growing *Quercus*, which eventually becomes dominant. Yet, there remain important gaps in our knowledge of the mechanism of competition, i.e. core process in succession, and synthetic ecosystem responses to climatic change, in particular the response of carbon dynamics.

To address the role of functional traits in competition and integrative ecosystem responses to climate change, we adopted a PFT-based ecosystem model and used our on-site measurements and the long-term studies at the Donglingshan (DLS) temperate forest watershed. Specifically, we tested two hypotheses: (1) differences in leaf physiological traits, derived from gas exchange measurements, and growth allometry between PFTs are possible mechanisms for competition and thus have the capacity to explain succession trends in temperate deciduous broadleaved forests; and (2) differences in ecophysiological traits and spatial configuration of habitats among PFTs within a landscape mosaic influence their responses to climate change in the past and the future.

MATERIALS AND METHODS

Study area

In eastern China, temperate deciduous broadleaved forests are distributed between 32°30′–42°30′N and 103°30′–124°10′E. Natural forests have virtually disappeared in lowland areas of the region (<1000 m a.s.l.) due to agricultural cultivation and economic development during the long history of the country's civilization. Remnant secondary forests after intensive human disturbance are found at mid-elevation (1000–2000 m a.s.l.) (Chen, 1997). The watershed of Donglingshan, hereafter referred as DLS, is located in the temperate forest zone, between 40°00′–40°02′N and 115°26′–115°30′E and occupying 21·3 km^2 (Fig. 1). The Beijing Forest Station of the long-term Chinese Ecosystem Research Network (CERN) is located at DLS. Elevation at DLS varies from 400 to 2000 m a.s.l. with an average of 1100 m (Fig. 1). The prevailing temperate semi-humid monsoon climate brings 500–600 mm of mean annual precipitation with a mean annual temperature of 2–8 °C (−10·1 °C in January and 18·3 °C in July) (Huang *et al.*, 1997; Fang *et al.*, 2006).

There are two major vegetation types within the DLS watershed: oak broadleaved forest (OAK) dominated by *Quercus liaotungensis*, mostly found on sunny slopes and currently occupying 32 % of the watershed; and birch/poplar forest (BIP) dominated by *Betula platyphylla* and *Populus davidiana*, occupying 10 % of the area, mostly on shadow slopes. Planted coniferous forest (CON, *Pinus tabulaeformis* and *Larix principis-rupprechtii*) occupies 7 % of the watershed (Ma *et al.*, 1997). Because of intensive human activity in the lowlands, about 41 % of the watershed has been degraded to shrubland, currently dominated by *Vitex negundo* var. *heterophylla* and *Pruns armeniaca* var. *ansu*. Crops are planted along riparian areas and represent 9 % of the watershed (Fig. 1).

Soils, classified according to soil development and physical and chemical characteristics of soil profiles, exhibit an altitudinal pattern (based on the 1 : 20 000 soil map, Sun, 1997). Mountain brown earths, mountain plaggen brown earths and mountain skeleton brown earths are found at mid-elevation. Luvic cinnamon soils, typical cinnamon soils, skeleton cinnamon soils and carbonate cinnamon soils are found at low elevation, while cultivated soils are found in the riparian areas (Fig. 1).

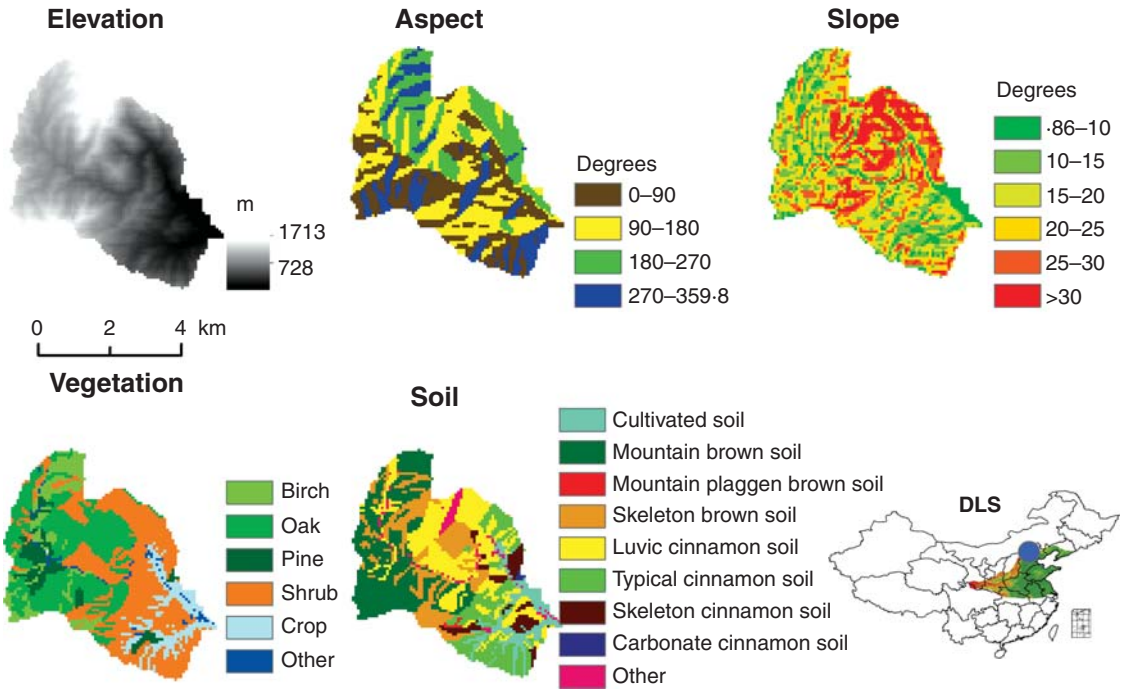

FIG. 1. Location, elevation, slope, aspect, current vegetation distribution and soil maps of the Donglingshan watershed (DLS).

Models and parameter estimation

We adopted the Terrestrial Ecosystem Simulator (TESim) in our investigation. TESim is a suite of process-based models simulating spatiotemporal ecosystem processes and vegetation dynamics at different scales, from spatially homogeneous patches (TESim-P) to heterogeneous landscapes (TESim-L) and regions (TESim-R) (Gao, 2006; Gao *et al.*, 2007). TESim also uses PFT-based approaches (multiple PFTs within one site) to simulate the spatiotemporal changes of ecosystem state variables (vegetation type, plant biomass, soil water and carbon/nitrogen in plant or soil), and interactions among the carbon, nitrogen and hydrological cycles, which are subject to various external environmental stresses, such as changes in climate, land use, grazing and harvesting intensities. In addition, spatial processes such as runoff–runon redistribution and re-absorption, and associated soil and nitrogen losses, are explicitly addressed in the TESim-L and TESim-R models (Gao *et al.*, 2007). These spatial processes make it necessary to load all the grid cells into the computer memory at the beginning of a TESim-L/R run instead of computing processes one pixel at a time. Plant pools include leaf, stem including branches, root and seed. Both structural and metabolic litter pools are simulated. Soil organic matter is divided into active and slow pools, and soil available nitrogen is also considered. Here we used four soil layers with a total depth of 1·8 m.

Carbon assimilation was calculated based on the assumptions that photosynthesis per leaf area is a hyperbolically increasing function of light intensity and intercellular CO_2 pressure, that intercellular CO_2 pressure is instantaneously determined by a balance between the inflow to stomata cavities and rate of photosynthesis, and that the mitochondrial respiration is an exponential function of temperature. The net carbon assimilation rate A_n (μmol CO_2 m^{-2} s^{-1}) for plants with C_3 carbon pathway is defined as follows (Thornley and Johnson, 1990; Gao *et al.*, 2004):

$$
\begin{aligned}
A_n &= [b - \sqrt{(b^2 + 4ac)}]/2a \\
a &= P_a(g_{so}g_x - g_{sc}g_p) \\
b &= g_{sc}g_{so}(\alpha_p I_p + g_x C_a + g_p O_a) - R_d a + \alpha_p I_p P_a(g_{sc}g_p + g_{so}g_x) \\
c &= g_{sc}g_{so}[R_d(\alpha_p I_p + g_x C_a + g_p O_a) + \alpha_p I_p(g_p O_a - g_x C_a)]
\end{aligned}
\qquad (1)
$$

where P_a is air pressure (kPa), I_p is light intensity (μmol m^{-2} s^{-1}), C_a and O_a are CO_2 and O_2 pressures on the leaf surface (kPa), respectively, g_{so} and g_{sc} are stomatal conductance (μmol m^{-2} s^{-1}) for O_2 and CO_2, respectively, α_p is photon efficiency, g_x and g_p are carboxylation conductance and photorespiration conductance (μmol m^{-2} s^{-1} kPa^{-1}), respectively, and R_d is dark respiration coefficient (μmol m^{-2} s^{-1}). The parameters α_p and g_x are considered to depend on leaf nitrogen content and temperature, and R_d is an exponential function of temperature (Medlyn *et al.*, 1999; Gao *et al.*, 2007).

The stomatal model is based on the assumptions that stomatal conductance is determined by leaf turgidity, that osmotic regulation is a hyperbolically increasing function of light intensity, and that water conductance from soil to leaf decreases with soil water stress. Thus, stomatal conductance g_s (mol H_2O m^{-2} s^{-1}) was computed as an increasing function of incident light intensity I_p, a decreasing function of vapour pressure deficit V_{pd} (kPa), CO_2 pressure on plant leaf C_a (kPa) and soil water potential ψ_s (MPa)

(Gao *et al.*, 2002, 2005).

$$g_s = \frac{b_g + \sqrt{b_g^2 + 4a_g c_g}}{2a_g}$$

$$a_g = r_z \frac{V_{pd}}{P_a} + \beta$$

$$b_g = \psi_s - \left(\beta + r_z \frac{V_{pd}}{P_a}\right) k_g + \pi_0 + \pi_p \left(\frac{C_0}{C_a}\right) \frac{I_p}{I_p + k_I}$$

$$c_g = k_g(\psi_s + \pi_0) \quad (2)$$

where β is the elastic modulus of guard cell structure (MPa m^2 s mol^{-1}), r_z is soil-to-leaf resistance (MPa m^2 s mol^{-1}), k_g is the half-saturation stomatal conductance (mol m^{-2} s^{-1}), k_I is the half-saturation light intensity (μmol m^{-2} s^{-1}), π_0 and π_p are the dark osmotic pressure and maximum light-inducible osmotic pressure (MPa), respectively, and C_0 is the reference CO_2 partial pressure (kPa).

Stomatal tolerance/resistance to soil and air moisture stresses is reflected in two synthetic indices: the possibly lowest soil water potential ψ_{min} that maintains open stomata:

$$\psi_{min} = -\pi_0 - \pi_p \left(\frac{I_p}{I_p + k_I}\right) \quad (3)$$

and the sensitivity of g_s to changes in V_{pd} at $C_a = C_0$:

$$S_v = \frac{\partial g_s}{\partial V_{pd}} = -\frac{g_s(g_s + k_g) r_z}{(2a_g g_s + b_g) P_a} \quad (4)$$

To parameterize TESim-P and TESim-L in this application, we used onsite measurements taken in summer 2006, as well as the long-term investigations carried out at this CERN station. Onsite leaf-gas-exchange flux for dominant species, measured with a Licor 6400 system (Licor Co., Lincoln, NE, USA) in 2006, was used to parameterize the leaf ecophysiological processes in TESim. Nutrient content of plants and soils, soil water, and soil texture were also measured in the field in 2006. In estimates of parameters at patch and landscape scales, we also used existing data from long-term investigations at this CERN station (www.cerndata.ac.cn) on community structure and biomass (Jiang, 1997), nutrients (Huang *et al.*, 1997), and soil physical and chemical characteristics (Sun, 1997). Finally, in the landscape-scale simulation, we adopted the default parameter values provided by TESim for shrubs and crops, for which we had neither field data nor literature sources. The parameters for allocation of assimilated materials and stomatal tolerance/resistance to water and moisture stresses are provided in Table 1.

The temporal resolution is 1 d for both TESim-P and TESim-L. For the simulations at the watershed scale, we used the 1 : 20 000 soil and vegetation maps produced by the Beijing Forest Station of CERN (www.cerndata.ac.cn) and the digital elevation model (DEM) map from the USGS (http://edc.usgs.gov) at a spatial resolution of 74 m. The soil and vegetation maps were converted to the same resolution as the DEM before analysis. Long-term daily meteorological records from Beijing station (39°48′N, 116°28′E, 1961–2001) were used as input drivers for the simulations at both patch and watershed scales, with temperature corrected based on the differences in elevation between the weather station and each studied grid cell.

Model evaluation

We used two independent local datasets for model evaluation of biomass, net primary productivity (NPP), respiration and littering. One dataset is the onsite long-term inventory on oak forest dynamics at a 30 × 40-m permanent plot from 1991 to 2002, in which individual basal area dbh (diameter at breast height) and canopy height were measured in 1991, 1997 and 2002 (Hou *et al.*, 2004). We applied the allometric equations developed on site to estimate biomass of leaf, stem/branch and root for the oak forest (Fang *et al.*, 2006), which were then compared with the simulated values. Annual NPP was calculated based on the biomass estimation for the period 1991–2002. Because the oak forest was estimated at around 80 years, but only 41 years of meteorological data from 1961 to 2001 were available, we repeated the 41-year data for the period 1920–1960 but with lower air CO_2 concentration according to historical CO_2 data (Keeling *et al.*, 2009), and used the assumed meteorological data for 1920–2001 to simulate oak forest dynamics with the TESim-P model. The simulated biomass and NPP for the period 1991–2001 were then compared with observations. A paired *t*-test was applied to evaluate the differences between simulations and observations (SAS Institute, 2002).

The other dataset comprises onsite measurements of biomass, litterfall, and estimated vegetation respiration and NPP for the oak forest, birch forest and pine forest in 1992–1994 (Fang *et al.*, 1995, 2006). The characteristics of the three plots, including elevation, slope, aspect and stand age,

TABLE 1. *Parameters on morphology and ecophysiology*

Symbol	Parameter	Units	BIP	OAK	CON	SHR
R_l	Partition coefficient for leaves	–	0·29	0·37	0·48	0·16
R_s	Partition coefficient for stems	–	0·63	0·44	0·36	0·53
R_r	Partition coefficient for roots	–	0·08	0·19	0·16	0·31
S_v	Sensitivity to air vapour	mol m^{-2} s^{-1} kPa^{-1}	−0·51	−0·37	−2·62	−1·04
ψ_{min}	Minimum soil water potential	MPa	−1·83	−2·71	−4·85	−3·08

BIP, birch/poplar forest; OAK, oak forest; CON, coniferous forest; SHR, shrubs. S_v was evaluated at I_p = 1·0 mmol m^{-2} s^{-1}, ψ_s = −0·05 MPa, V_{pd} = 1 kPa and P_a = 101·3 kPa.

were used in TESim-P. Simulated total biomass, stem/branch biomass, leaf biomass, NPP, net increment in biomass, litterfall and vegetation respiration were compared with observations. NPP was assumed to equal the sum of litterfall and net increment in biomass in the calculation. A paired *t*-test was also applied to detect differences between simulations and observations.

Simulations and predictions

To test whether the model can simulate the competition between OAK and BIP and the consequent succession, TESim-P was run for 82 years by repeating the 41-year climate from 1961 to 2001, with the assumption that the seeds and seedlings of both OAK and BIP were available in the stand at the initial stage. To separate the effects of competition between OAK and BIP on ecosystem functions, we designed a comparative scenario keeping the two forests in different stands without interspecific interaction, while assuming the same climate and soil conditions as the previous competition scenario.

We then ran TESim-L to simulate water and carbon dynamics of the watershed for the period 1961–2001. To predict changes in carbon balance of the DLS watershed in the context of global climate change, a future climate scenario was prescribed by extrapolating the increasing trends of temperatures experienced in the 41 years 1961–2001. Slopes of increases in the daily minimum, mean and maximum temperatures were determined by applying regression analysis on the daily climate data for 1961–2001. Differences in carbon and water dynamics between the past and the future scenario with temperature increases were analysed at the watershed scale.

RESULTS

Model evaluation

Mean values of leaf, stem/branch and root biomass, and NPP were not significantly different between the simulations and the observations for the oak forest permanent plot with a stand age of 80 years (Fig. 2, paired *t*-test, $P < 0{\cdot}05$). In comparison with the *in situ* field measurements during August 1992 to July 1994 (Fang *et al.*, 1995, 2006) in the oak, birch and pine forests, there was no significant difference between the simulations and the observations for total, stem/branch, NPP, litterfall, and vegetation respiration for any of the three forests (Fig. 2, paired *t*-test, $P < 0{\cdot}05$).

Carbon dynamics for the two forest patches without competition

Annual NPP of the two deciduous broadleaved forests followed the interannual variations of annual precipitation (Fig. 3, BIP only, OAK only). Mean NPP was 518·4 g m^{-2} yr^{-1} for OAK forest and 441·7 g m^{-2} yr^{-1} for BIP forest. For the period 1991–2001, mean NPP was 667·2 g m^{-2} yr^{-1} for OAK forest and 685·3 g m^{-2} yr^{-1} for BIP forest. Without competition with OAK, the BIP forest was able to store 9·8 kg m^{-2} dry biomass in the trunk and branches after 40 years, whereas the OAK forest was able to store only about 6·8 kg m^{-2} dry biomass in the trunk and branches, i.e. about 30 % less.

Competition between OAK and BIP communities

When considering competition between OAK and BIP (Fig. 3, BIP in combined, OAK in combined), during the first 10 years of the succession, NPP of BIP (250 g m^{-2} yr^{-1}) was twice that of OAK (120 g m^{-2} yr^{-1}). After the initial 10 years, OAK had higher NPP than BIP. Similarly, the root biomass of BIP (mean 200 g m^{-2}) was higher than that of OAK (147 g m^{-2}) for the initial 15 years, but then got lower. BIP maintained higher stem/branch biomass than OAK over the initial 25 years (mean 1344 g m^{-2} for BIP vs. 701 g m^{-2} for OAK), but following this the reverse was the case. The stem/branch biomass of BIP declined rapidly after 40 years from 1647 to 743 g m^{-2} in year 50.

Carbon and water dynamics of the watershed and their responses to climatic change

Simulated mean annual transpiration and evaporation for the whole watershed were 37 $\pm$ 11 and 8 $\pm$ 3 cm yr^{-1}, respectively, for the period 1961–2001 (Fig. 4). The three forests had similar mean annual transpiration, with the highest of 47 $\pm$ 15 cm yr^{-1} for BIP and lowest of 45 $\pm$ 12 cm yr^{-1} for CON. Simulated mean annual evaporation was 4·5 cm yr^{-1} for BIP, 5·9 cm yr^{-1} for OAK, 7·4 cm yr^{-1} for CON and 8·9 cm yr^{-1} for shrubs (SHR). Simulated watershed-averaged NPP was 287 gC m^{-2} yr^{-1}, litter mass was 338 g m^{-2} and heterotrophic respiration was 121 gC m^{-2} yr^{-1} (Fig. 4, Table 2).

Daily minimum, maximum and mean temperatures in the meteorological records for 1961–2001 showed significant increasing slopes of 0·0678, 0·0201 and 0·047 °C yr^{-1}, implying that they had increased by 2·78, 0·82 and 1·93 °C over the 41 years, respectively. However, annual precipitation fluctuated between a minimum of 256 mm in 1965 and a maximum of 894 mm in 1969 without any significant increasing or decreasing trend for 1961–2001 (Fig. 5). These trends of climate variation were extrapolated to form the future scenario for the next 41 years after 2001.

This future scenario with increased temperature resulted in an increase of average NPP (+19 %), heterotrophic respiration (+23 %) and plant carbon storage (+28 %) in the watershed. Average evapotranspiration and net ecosystem carbon balance of the watershed increased by 3 and 17 %, respectively. The watershed average litter mass showed little change (Table 2, Fig. 4).

The increase in temperature also resulted in different changes in state and flux variables of the plant functional types within the watershed. NPP of OAK, BIP and CON increased by 19, 33 and 25 %, respectively. Litter mass of BIP increased by 8 %, but that for OAK and CON decreased slightly by 3 and 2 %, respectively.

DISUSSION

Model evaluation

Complete evaluation of the process-based and spatially explicit simulations across broad spatial and temporal scales remains a challenge (Rastetter, 1996; Perry and Enright, 2006; Scheller and Mladenoff, 2007). Most of the processes incorporated in

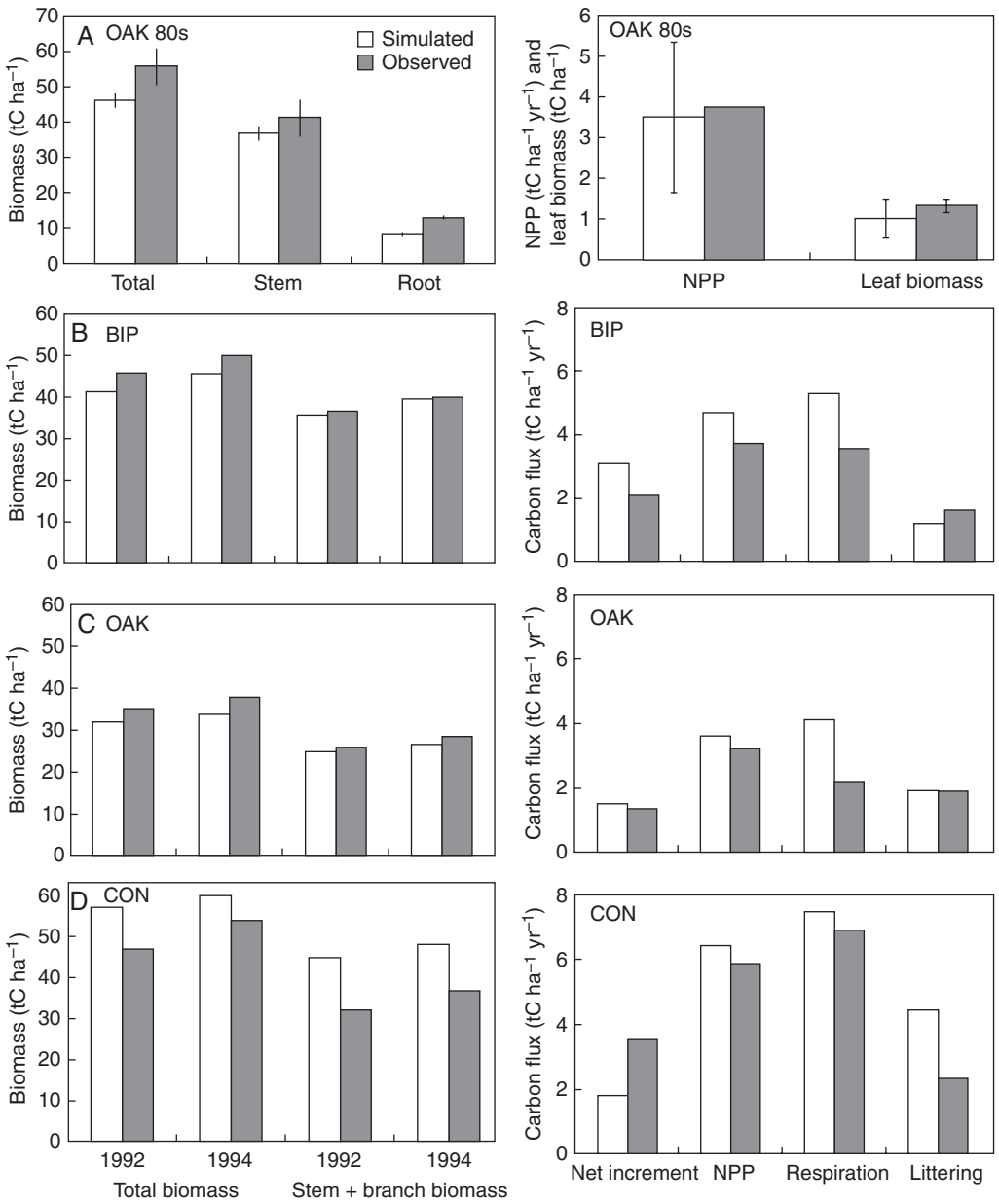

FIG. 2. Comparisons between observed and simulated vegetation variables at the permanent 80-year-old oak plot (A), and the plots for 4-year period (1992–1994) for the oak forest (B), birch forest (C) and pine forest (D). NPP, net primary productivity.

the models are difficult to replicate in reality at either spatial or temporal scales (Perry and Enright, 2006). There are no complete spatiotemporal data existing in this study for sufficient evaluation. However, long-term investigations at typical sites, such as those of the LTER (Long Term Ecological Research network) in the United States (www.lternet.edu) and CERN in China, may provide evidence and data to allow indirect and partial evaluation. We used two independent data sets, from long-term investigations at the Beijing Forest Ecosystem Station of CERN, to evaluate biomass and carbon dynamics of three typical forests at the patch scale. The model is robust in simulating biomass dynamics and allocation, NPP and vegetation respiration for the three typical forests (Fig. 2).

Competition

The present study supports the hypothesis that the ecophysiological traits and growth allometry of PFTs can explain the interspecific competition and consequent succession trends observed in the temperate deciduous forests of China. Community succession direction is a result of competition, yet is subject to various disturbances, especially the increasingly intensive human disturbance. The consequent changes in ecosystem composition/structure may significantly alter the responses and feedbacks of the carbon, water and nutrient dynamics to climate change (Field *et al.*, 2007). It is critical for coupled biogeochemical and biogeographical models to address these correctly in the simulations to give scientifically

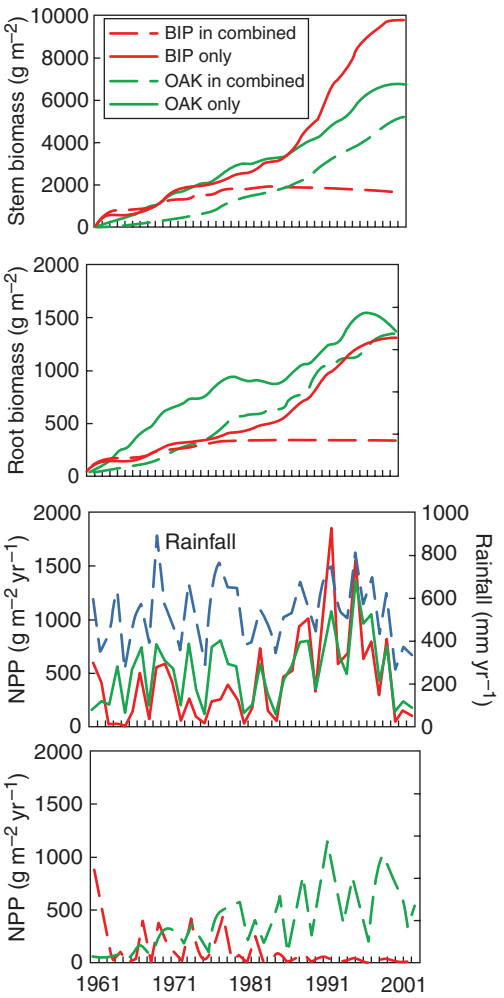

FIG. 3. Simulations of net primary productivity (NPP) and biomass dynamics for BIP and OAK forests with (BIP or OAK in combined) and without competition (BIP or OAK only). Mean annual precipitation is indicated.

sound predictions in the context of global change. Although competition between OAK and BIP and the succession from BIP to OAK have been described in the literature, simulations of the competition based on ecophysiology and associated in-depth analysis of the mechanisms are seldom reported.

In our simulation, the differences in drought resistance and tolerance and biomass allocation incorporated in the simulation model were the key factors for competition and for the onset of subsequent succession between the two plant functional types. As competition continues, morphological factors, as the consequence of difference in allocation of biomass, then contribute. The leafy OAK tends to allocate more carbon to leaf and root than BIP, as reflected in the model parameter indicating production allocation to leaf, 0·37 for OAK and 0·29 for BIP (Table 1). By contrast, BIP has been known to have greater per-leaf-area productivity when soil resources are abundant at the initial stage of succession, and it can accumulate biomass in stem and grow quickly, in agreement with higher NPP and biomass for BIP than for OAK in our simulation. The BIP-dominated state lasts until 20–30 years (Fig. 3). After this initial period of succession, BIP declines quickly and OAK becomes dominant as soil water decreases, because OAK trees are more resistant and tolerant to soil moisture stress during the competition for soil moisture. The leafy OAK trees then further block the light for BIP to regenerate.

The drought tolerance of a PFT is reflected by the parameter in our stomatal conductance model: the theoretically allowable minimum soil water potential ψ_{min} (eqn 3, Table 1). This parameter, signifying the tolerance of plants to soil water stress (Gao *et al.*, 2007), is estimated as −2·71 MPa for OAK and −1·83 MPa for BIP. This means that OAK can endure greater soil water stress and remain active metabolism more easily than BIP. OAK also has lower stomatal sensitivity (eqn 4, Table 1) to variations in vapour pressure deficit, −0·37 mol m^{-2} s^{-1} kPa^{-1}, than the corresponding sensitivity of the BIP functional type, −0·51 mol m^{-2} s^{-1} kPa^{-1}, both

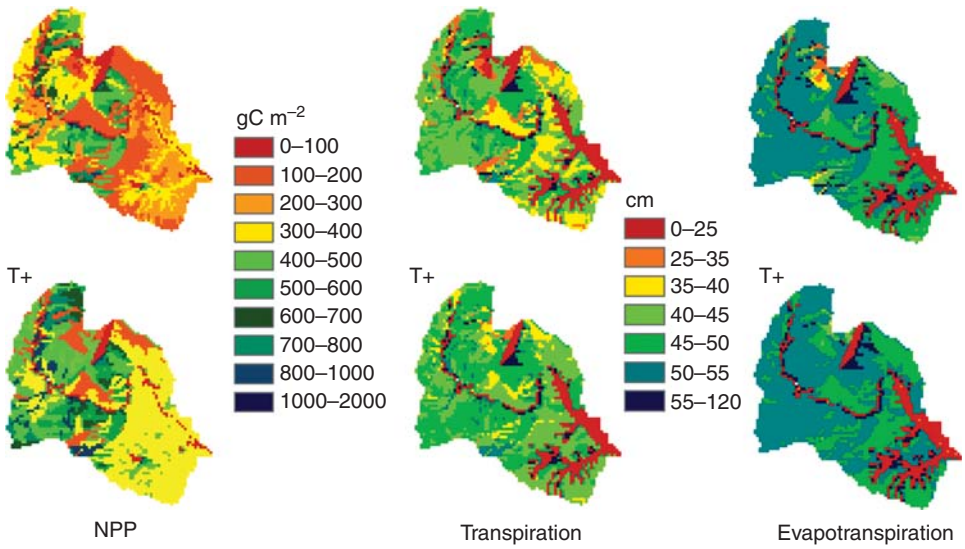

FIG. 4. NPP, transpiration and evapotranspiration of the Donglingshan watershed under the current climate (top) and the warming climate (T +, below) scenarios.

TABLE 2. *Simulations of carbon and water dynamics for the period 1961–2000 (current scenario) and the future scenario with increased temperature.*

Variable	Current/future scenario				
	Watershed	OAK	BIP	CON	SHR
NPP	287/342	408/485	486/647	249/311	182/220
CPT	2123/2721	3532/4297	6178/8426	1558/2006	824/1110
MLT	338/338	527/513	384/415	522/511	259/264
CRS	121/149	167/200	125/165	129/160	122/150
NEP	165/193	241/285	361/482	120/151	60/70
TRN	370/395	461/475	468/482	450/467	383/429
EVP	81/70	59/48	45/32	74/62	89/73

NPP, net primary productivity (gC m^{-2} yr^{-1}); CPT, carbon stored in plants (gC m^{-2}); MLT, litter mass (g m^{-2}); CRS, heterotrophic respiration (gC m^{-2} yr^{-1}); NEP, net ecosystem production (gC m^{-2} yr^{-1}); TRN, transpiration (mm yr^{-1}); EVP, evaporation (mm yr^{-1}).

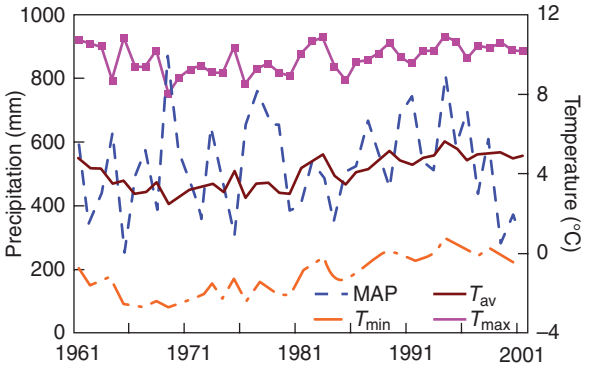

FIG. 5. The dynamics of annual minimum (T_{min}), average ($T_{av.}$), maximum temperature (T_{max}) and mean annual precipitation (MAP) between 1961 and 2001.

evaluated at $\psi_s = -0{\cdot}05$ MPa, $I_p = 1$ mmol m^{-2} s^{-1} and $V_{pd}/P_a = 0{\cdot}01$. These values show that although BIP has greater stomatal conductance in the wet, its high stomatal sensitivity to soil and air moisture stresses brings its stomata to closure as soil or air water stress intensifies.

The greater drought tolerance and resistance of OAK than BIP were also observed in the intensive hydro-physiological measurements using pressure–volume curve analysis (Li and Chen, 1997*a*). The reported mean lowest leaf water potential, $\psi_{l,min}$, during a growth season is −1·59 MPa for OAK compared with −1·32 MPa for BIP. Mean leaf osmotic potential at plasmolysis, $\psi_{l,tip}$, is −2·63 MPa for OAK versus −2·04 MPa for BIP. Maximum leaf cell elastic modulus ε_{max}, signifying cell stiffness and partly representing the ability to keep stomata open during water stress, is 19·1 MPa for OAK and 15·8 MPa for BIP. The capacity for osmotic adjustment is closely related to the difference between the maximum osmotic potential at saturation and $\psi_{l,tip}$, and the difference between the diurnal maximum and minimum leaf water potential. Li and Chen (1997*a*) reported first and second differences for OAK of 0·73 and 1·84 MPa, respectively, in comparison with 0·54 and 1·25 MPa for BIP. Time-series analysis of stem sap-flow also concluded that OAK had greater capability than BIP in self-stabilizing stem sap-flow during environmental changes (Li and Chen, 1997*b*). All these independent measurements support our parameter estimates, and that OAK has greater tolerance and resistance to moisture stresses than BIP (Tyree, 1976; Li and Chen, 1997*a*; Gao *et al.*, 2002).

A sensitivity analysis was designed to investigate the sensitivities of competition to the coefficients of allocation for roots and leaves, R_r and R_l, and the maximum osmotic pressure of leaves, $\pi = \pi_0 + \pi_p$, which signifies the stomata tolerance to water stress. Variation of each of the parameters was designed in a complementary way so that increases in one parameter for OAK were always accompanied by decreases in the same parameter for BIP. The variation ranges of the parameter were chosen so that the difference of the parameter between OAK and BIP was approximately reversed. In other words, if a parameter takes values of p_1 and p_2 for OAK and BIP, respectively, variation of the parameter in the sensitivity analysis will allow OAK and BIP to exchange parameter values so that OAK will take the value p_2 and BIP will take the value p_1. This design will allow us to compare the sensitivities to the three parameters. Finally, because π is the sum of π_0 and π_p, variation of π in the sensitivity analysis necessitated the conserved ratio of π_0/π_p. Calculation of average stem biomass over 80 years of simulation for the designed parameter sets showed that increased allocation for roots and leaves and maximum osmotic pressures of BIP, accompanied by a decrease in these parameters of OAK, all led to increased average stem biomass of BIP but decreased stem biomass of OAK (Fig. 6). Average stem biomass was more sensitive to maximum osmotic pressure and allocation for leaves than to allocation for roots. Leaves contribute directly to carbon assimilation and growth and maximum osmotic pressure determines stomatal conductance and assimilation rates under water stresses, whereas the effect of variation in allocation to roots is indirect.

Landscape responses

The TESim simulations illustrate the possible ecosystem responses to climate change in the DLS watershed, and the results support the hypothesis that the differences in ecophysiological traits and habitat spatial configurations of PFTs influence their responses to climate change.

The impacts of increased temperature on NPP and carbon stocks in plants of the whole watershed are positive, despite the increased respiration and soil water stress (Table 2). The

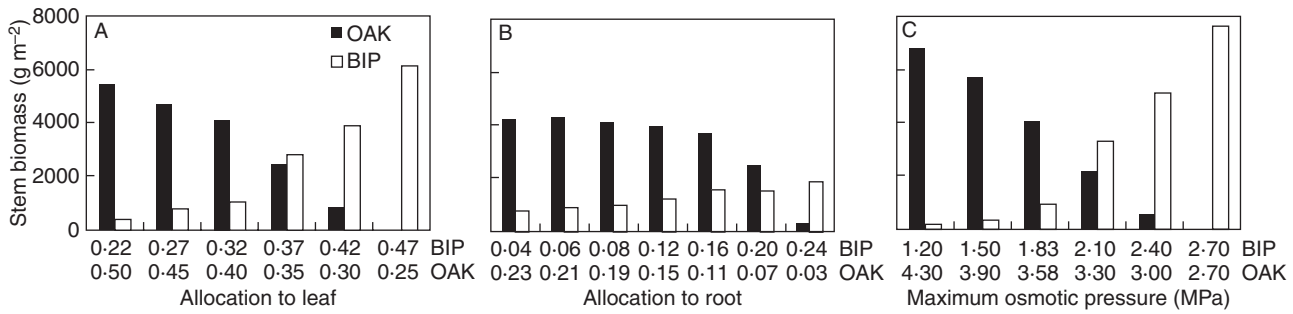

FIG. 6. Sensitivity of average stem biomass in competition between BIP and OAK to carbon allocation for leaves (A), roots (B) and maximum osmotic pressure (C). Stem biomass was averaged across the simulation period.

positive effects include overall enhanced assimilation and reduced evaporation that partially offset the temperature-induced increase in potential transpiration. These positive temperature effects might have something to do with the mountainous forests in this study, for which temperature is an important limitation to the length of the growing season as well as activities of the plants and microbes.

However, the responses to increased temperature differ among various forests due to their different habitat occupation and intrinsic ecophysiological characteristics. In this temperate watershed, BIP currently occupies habitats with the highest elevation (around 1200 m) and lowest mean annual temperature (MAT, 7·15 °C), while OAK is mostly located at 1000 m with MAT of 7·8 °C, and CON trees are mostly found at 800 m with MAT of 8·37 °C. The difference in MAT might have contributed to the difference in evaporation (Table 2) and volumetric soil water content (WS). Our simulation gave average annual WS of 0·25 and 0·21 for the first and second soil layers of BIP, respectively, compared with 0·2 and 0·15 for OAK, and 0·18 and 0·13 for CON. In addition to the difference in habitat locations, the BIP, with its high productivity and high sensitivity to environmental changes, also showed the highest gain (33 %) in NPP compared with OAK (19 %) and CON (25 %) under the increased temperature scenario (Table 2).

Current litter mass is the result of a dynamic balance between litter production and decomposition. Increased temperature brought about more source biomass of litter production, but also accelerated the litter loss by increased decomposition rate. By contrast, increased evapotranspiration may substantially decrease soil moisture and subsequently decomposition rate, thus contributing to litter accumulation. Simulated average litter mass of the whole watershed remained almost unchanged with respect to the temperature increase, indicating the close balance between these effects. However, the average litter mass of BIP increased by 7 % partly because it occupied a higher elevation with lower baseline temperature, and the increase in litter production predominated. The slightly decreased litter biomass of OAK and CON can be explained by the lower and warmer locations where the effect of increased temperature on decomposition prevails.

Disturbance, an important driver of secondary succession, is an increasingly important topic because of intensified human activities, such as land-use change, and the changes in disturbance regimes resulting from climate change (Turner *et al.*, 1998; Perry and Enright, 2006; Scheller and Mladenoff, 2007). It is vital to incorporate disturbance and consequent secondary succession in the ecosystem trajectories in future climatic change/land-use change scenarios. Here we have successfully quantified an important secondary succession path in a temperate forest based on the traits of stomatal behaviour and biomass allocation strategies of the two dominant plant functional types involved, by ecosystem simulation modelling. The simulation yielded substantial changes in carbon fluxes and ecosystem structure during secondary succession. These ecophysiological traits also contributed to our understanding of different responses of PFTs in a landscape mosaic to future climate change.

ACKNOWLEDGEMENTS

This work was supported by the National Natural Science Foundation of China (30590384) and Chinese Academy of Sciences (KZCX2-YW-430-07). We thank Dr C. Zhou and Mr M. Dong for help with fieldwork and Dr S. Zhang for sharing his work on ecophysiology.

LITERATURE CITED

Bachelet D, Lenihan JM, Daly C, Neilson RP, Ojima DS, Parton WJ. 2001. *MC1: A dynamic vegetation model for estimating the distribution of vegetation and associated ecosystem fluxes of carbon, nutrients, and water*. Version 1·0. General Technical Report PNW-GTR-508. Portland, OR: US Department of Agriculture, Forest Service, Pacific Northwest Research Station.

Baker WL. 1999. Spatial simulation of the effects of human and natural disturbance regimes on landscape structure. In: Mladenoff DJ, Baker WL. eds. *Spatial modeling of forest landscapes: approaches and applications*. Cambridge: Cambridge University Press, 277–309.

Beard KH, Vogt KA, Vogt DJ *et al.* 2005. Structural and functional responses of a subtropical forest to 10 years of hurricanes and droughts. *Ecological Monographs* **75**: 345–361.

Bond-Lamberty B, Gower ST, Ahl DE, Thornton PE. 2005. Reimplementation of the Biome-BGC model to simulate successional change. *Tree Physiology* **25**: 413–424.

Botta A, Foley JA. 2002. Effects of climate variability and disturbances on the Amazonian terrestrial ecosystems dynamics. *Global Biogeochemical Cycles* **16**: v1070. doi:10.1029/2000GB001338.

Bugmann H. 2001. A review of forest gap models. *Climatic Change* **51**: 259–305.

Chen L. 1997. The importance of Dongling Mountain region of warm temperate deciduous broad-leaved forest. In: Chen L, Huang J. eds. *Studies on the structures and functions of the warm-temperate forest ecosystems*. Beijing: Science Press, 8–25.

Dale VH, Joyce LA, McNulty S, Neilson RP, Ayres MP. 2001. Climate change and forest disturbances. *Bioscience* **51**: 723–734.

Elmore AJ, Mustard JF, Hamburg SP, Manning SJ. 2006. Agricultural legacies in the great basin alter vegetation cover, composition, and response to precipitation. *Ecosystems* **9**: 1231–1241.

Fang J, Wang X, Liu G, Kang D. 1995. Measurement of respiration amount of trees in *Quercus liaotungensis* community. *Acta Ecologica Sinica* **15**: 235–244.

Fang J, Liu G, Zhu B, Wang X, Liu S. 2006. Carbon cycles of three temperate forest ecosystems in Dongling Mountain, Beijing. *Science in China Series D-Earth Sciences* **36**: 533–543.

Field CB, Lobell DB, Peters HA, Chiariello NR. 2007. Feedbacks of terrestrial ecosystems to climate change. *Annual Review of Environment and Resources* **32**: 1–29.

Friend AD, Schugart HH, Running SW. 1993. A physiology-based gap model of forest dynamics. *Ecology* **74**: 792–797.

Gao Q. 2006. *Terrestrial Ecosystem Simulator (TESim) User's Guide*. Beijing: Beijing Normal University.

Gao Q, Zhao P, Zeng X, Cai X, Shen W. 2002. A model of stomatal conductance to quantify the relationship between leaf transpiration, microclimate and soil water stress. *Plant Cell Environment* **25**: 1373–1381.

Gao Q, Zhang XS, Huang YM, Xu HM. 2004. A comparative analysis of four models of photosynthesis for 11 species in the Loess Plateau. *Agricultural and Forest Meteorology* **126**: 203–222.

Gao Q, Yu M, Zhang XS, Xu HM, Huang YM. 2005. Modelling seasonal and diurnal dynamics of stomatal conductance of plants in a semiarid environment. *Functional Plant Biology* **32**: 583–598.

Gao Q, Yu M, Liu Y, Xu H, Xu X. 2007. Modeling interplay between regional net ecosystem carbon balance and soil erosion for a crop-pasture region. *Journal of Geophysical Research-Biogeosciences* **112**: G04005. doi:10.1029/2007JG000455.

He HS, Mladenoff DJ. 1999. Spatially explicit and stochastic simulation of forest-landscape fire disturbance and succession. *Ecology* **80**: 81–99.

Hou J, Huang J, Ma KP. 2004. Eleven-year population growth dynamics of major species in a *Quercus liaotungensis* forest in the Dongling Mountains of Northern China. *Acta Phytoecologica Sinica* **28**: 609–615.

Huang J, Kong F, Jiang H. 1997. The characteristics of the nutrient accumulation of the arboreous layer of deciduous broad-leaved forests in Dongling Mountain, Beijing. In: Chen L, Huang J. eds. *Studies on the structures and functions of warm-temperate forest ecosystems*. Beijing: Science Press, 270–294.

Jiang H. 1997. Study on biomass of *Quercus liaotungensis* and *Betula dahurica* forest in Dongling Mountain. In: Chen L, Huang J. eds. *Studies on the structures and functions of warm-termperate forest ecosystems*. Beijing: Science Press, 115–134.

Keane RE, Cary GJ, Davies ID *et al*. 2004. A classification of landscape fire succession models: spatial simulations of fire and vegetation dynamics. *Ecological Modelling* **179**: 3–27.

Keeling RF, Piper SC, Bollenbacher AF, Walker JS. 2009. Atmospheric CO_2 records from sites in the SIO air sampling network. In: *Trends: A compendium of data on global change*. Oak Ridge, TN: Carbon Dioxide Information Analysis Center, Oak Ridge National Laboratory, US Department of Energy.

Lecomte N, Simard M, Fenton N, Bergeron Y. 2006. Fire severity and long-term ecosystem biomass dynamics in coniferous boreal forests of eastern Canada. *Ecosystems* **9**: 1215–1230.

Li H, Chen L. 1997*a*. Study on the hydro-physiological characteristics of major plant species of the forest ecosystem in the warm temperate zone of Northern China. In: Chen L, Huang J. eds. *Studies on the structures and functions of warm-temperate forest ecosystems*. Beijing: Science Press, 238–263.

Li H, Chen L. 1997*b*. Study on the water flux of major tree species and the canopy transpiration in warm temperate mountainous forest ecosystems. In: Chen L, Huang J. eds. *Studies on the structures and functions of warm-temperate forest ecosystems*. Beijing: Science Press, 264–269.

Luo Y. 2007. Terrestrial carbon-cycle feedback to climate warming. *Annual Review of Ecology, Evolution, and Systematics* **38**: 683–712.

Ma KP, Chen L, Yu S, Huang J, Gao X, Liu C. 1997. The major community types in Dongling Mountain region. In: Chen L, Huang J. eds. *Studies on the structures and functions of warm-temperate forest ecosystems*. Beijing: Science Press, 56–75.

Medlyn BE, Badeck FW, De Pury DGG *et al*. 1999. Effects of elevated $[CO_2]$ on photosynthesis in European forest species: a meta-analysis of model parameters. *Plant Cell Environment* **22**: 1475–1495.

Mladenoff DJ. 2004. LANDIS and forest landscape models. *Ecological Modelling* **180**: 7–19.

Parton WJ, Scurlock JMO, Ojima DS *et al*. 1993. Observations and modeling of biomass and soil organic-matter dynamics for the grassland biome worldwide. *Global Biogeochemical Cycles* **7**: 785–809.

Perry GLW, Enright NJ. 2006. Spatial modelling of vegetation change in dynamic landscapes: a review of methods and applications. *Progress in Physical Geography* **30**: 47–72.

Rastetter EB. 1996. Validating models of ecosystem response to global change. *Bioscience* **46**: 190–198.

Scheller RM, Mladenoff DJ. 2007. An ecological classification of forest landscape simulation models: tools and strategies for understanding broad-scale forested ecosystems. *Landscape Ecology* **22**: 491–505.

Shugart HH, Smith TM. 1996. A review of forest patch models and their application to global change research. *Climatic Change* **34**: 131–153.

Sun S. 1997. The characteristics of the geology, geomorphology, and soils in Dongling Mountain region. In: Chen L, Huang J. eds. *Studies on the structures and functions of warm-temperate forest ecosystems*. Beijing: Science Press, 10–27.

Thornley JHM, Johnson IR. 1990. *Plant and crop modelling*. Oxford: Clarendon Press.

Thornton PE. 2000. *User's Guide for Biome-BGC, Version 4·1·1*. University of Montana, Missoula, MT: Numerical Terradynamic Simulation Group, School of Forestry.

Turner MG, Baker WL, Peterson CJ, Peet RK. 1998. Factors influencing succession: lessons from large, infrequent natural disturbances. *Ecosystems* **1**: 511–523.

Tyree MT. 1976. Physical parameters of the soil-plant-atmosphere system: breeding for drought resistance characteristics that might improve wood yield. In: Connell MGR, Last PT. eds. *Tree physiology and yield improvement*. London: Academic Press, 329–348.